_____

Performance Comparison of TR and FSRUWB System Using Particle Filter: Effects of Frequency, Data Rate, Multi-Path and Multi-Channel Communication

¹Vishal B. Raskar, ²Swapnil L. Lahudkar
¹Research Scholar, Department of Electronics & Telecommunication Engineering,
JSPM's Rajarshi Shahu College of Engineering, Tathawade,
Pune, India.
raskarvishal2013@gmail.com
²Professor, Department of Electronics & Telecommunication Engineering,
JSPM's Imperial College of Engineering & Research, Wagholi,
Pune, India.
swapnillahudkar@gmail.com

Abstract—In this study, we introduced a novel scheme based on Transmitted References (TR) and Frequency Shifted Reference (FSR) for ultra-wideband (UWB) system. By taking into account tracking loop-based particle filtering together with a data collecting approach for single and multi-path channel situations, the suggested method is an enhanced model. Each particle's location is determined using this filtering technique, which is then utilised to calculate the timing inaccuracy and regulate the UWB system's timing pulse. Also, it can tackle the multimodal distribution of errors then effectively approximate the optimal solution. The data distribution is discretised via a number of particles that are weighted samples evolving concerning time duration. The simulation results show that, in terms of error rate, number of particles, and delay response, the recommended model of FSR-UWB with particle filter performs better than the TR-UWB with and without considering particle filter.

Keywords-Communication system, transmitted and frequency-shifted reference ultra-wideband, multi-path channels.

I. INTRODUCTION

WSN has numerous applications in Intelligent Vehicular Systems, military sensing, data broadcasting, multimedia, environmental monitoring, agriculture, patient monitoring, industrial automation, etc. But it has some limitation such as smaller storage device, very low battery power, lower computing power, and narrow network bandwidth. A new MAC protocol is designed, and it named Wide-MAC for WSN by using ultra-wideband Impulse Radio (IR-UWB) transceivers. This system's key benefit is its lower power consumption, which is comparable to the energy consumption model for IR UWB-based transceivers [1]. Ultra-wideband is the guarantee technology for low complexity, low power and short distance communication. UWB system is an alternate potential way to a traditional communication system specific to the low power and short-range wireless applications [2].

The significance of the wideband system offers a vast diversity in frequency for combating multiple path fading, high data rates, mitigates both non-system and multiuser interference. But the enormous bandwidth of UWB systems creates a system more complicated in the conventional UWB system, which employs either pulse-position modulation or antipodal with extremely short duration pulses. Also, the UWB system limits the system performance such as BER, throughput, and node flexibility in UWB receiver design. These challenges may be led to synchronization errors [3]. In order to solve the receiver complexity issues, impulse-based UWB system that specific to the low-data-rate systems via transmitted reference (TR) UWB system [4, 5] and frequency-shifted reference (FSR) UWB system; but synchronization and timing error has not been considered. The present study has overcome the shortcomings of traditional suggested solutions and investigates and designs a new UWB system for efficient synchronization and fine timing at low transmit power. Also, a particle filter is utilized with an acquisition method for multipath channel conditions. The various bands and wireless sensor networks are briefly described in this section. The next

269

_____

section discussed the related work and gives a research gap. Section 3 discusses the methodology with respect to the timing acquisition, TR and FSR. Section 4 gives the results for the work with and without particle filter and has discussed the results. The final chapter concludes the entire research.

II. RELATED WORK

Presently, many researchers have attracted the impulse radio ultra-wideband (UWB) technology to apply position location and different communication purposes [6]. The UWB includes some properties such as high penetrability, fine time resolution, and low fading margin in dense multi-path and low probability of intercept. Moreover, it used numerous applications, which led to a rise in the government agencies and companies working in UWB [7]. In traditional, most of the designing of UWB is used in indoor environment applications. The indoor UWB system comprises several channels for characterising numerous resolvable multi-path components [8],and the UWB pulse duration is shorter than the magnitude of delay spreads. The UWB transmission provides the possible user location accurately for transmitting the synchronised data, power, traffic routed data, and rate allocation in a wireless ad hoc environment. The challenges are limit the system performance such as BER, throughput, and node flexibility in UWB receiver design. These challenges may be led to synchronisation errors [3]. Particularly the signal detection process, interference mitigation and synchronisation error in the UWB system.

On the other hand, a study by Huo et al. [9] have proposed a model for the UWB transmitter, which provides the modulation scheme of the new Transmitted-Reference Pulse-Cluster (TRPC). The simulated results show that variable data-rate is obtained for a significant operating frequency between 10 and 300 Mbps, with effective sideband suppression, reduced carrier-leakage, and linearity, thereby achieving efficient energy efficiency and consuming low power. Research by Liang et al. [10] has also presented TRPC signalling and developed for non-coherent UWB communications. The simulated results show that the suggested model's carrier frequency offset remains constant. Using a pass-band transmitter and a non-coherent receiver also demonstrates how phase offset may be removed. Moreover, a semi-analytical BER derivation has been obtained to show the effect of phase noise on system error performance. It is seen from the results that the proposed method is better than the traditional TR and coherent UWB Rake receivers.

A study by Djapic et al. [11] presented a synchronisation approach for multiple user TR-UWB systems. The suggested model distributes data packet offsets with a better resolution by analysing the blocks containing the transmitted data. The complicated algorithm is simplified by using the right property. The complete transceiver data sequence is considered along with the obtained channel impulses for a university structure. When the number of users is increased, the performance is improved. By choosing the user codes with reduced cross-correlation qualities across all code offsets, the issue may be resolved. Also, a study by Franz and Mitra,[12] Yi-Ling Chao & Scholtz,[13], reported that the conventional TR-UWB system is complex for building on lower power applications for TR UWB receiver. For normal TR-UWB, the delay element must thus be avoided [14].S. L. Bangare et al. [28-30] worked in the disciplines of ML and IoT also for code parser. S. Gupta et al. [31] demonstrated effective extraction techniques. Campus navigator work proposed by P. S. Bangare et al. et al. [32]. The network security work was proposed by Xu Wu et al. [33]. Deep neural networks were employed well for brain tumor research by A. S. Ladkat et al. [34]. L.M.I. Leo Joseph et al. [35] proposed use of the Deep learning.To overcome the above issues like interference mitigation, synchronisation error, throughput, time delay in conventional UWB system, we are implementing the frequency translation of a wideband signal with an adaptation of particle filter in both TR-UWB and FSR-UWB that is simple when relating to the delay of the same signal. On the other hand, in the frequency domain, the references are translated relatively concerning time orthogonal to the data-bearing signals and attain a small frequency shift. This recognises the orthogonality of data and reference signals for a sample period. Henceforth the frequency offset among the data and reference impulse trains is modelled in the inversed symbol period. This shift in the frequency is less than the frequency coherence of channels; hence, the references are compatible with low data rate applications as desired.

III. PARAGRAPHS & ITEMISATIONS

Initially, the input parameters are initialised in the UWB system, including a dynamic array of particle states, number of particles, numerical fusion positioning result, noise variance, weight array and particle score. Then particle weight is calculated based on acquired value from the collected UWB data. Generally, the particle filter is used for estimating the state of dynamic system performance. A person's position and velocity in the UWB system are represented by the state x_t, i.e., $x_t = [x_t, y_t, z_t, v_{xt}, v_{yt}, v_{zt}]$. The particle utilises the N particles, which denotes various possible conditions toward estimate this state level. The acceleration and velocity of each particle are set to zero, and particle position spread over a test area. Subsequently, the condition of every particle is updated along with the movement models. In this regards, particles with more weight are measured. At last, the particles are resampled which means that new particle sets will be selected on the basis of old set whereas, heavier particles have more

_____

chance of appearing multiple times in this new set.

Algorithm 1: Particle filter
Initialise particles
while true do
Update particles with the movement model
Determine weight for every particle based on the UWB measurement
Return the particle with the highest weight
Resample
end while

In order to model the particle movement, distinct time-noise accelerating model has been utilised for x_t:

$$x_{l+1} = Fx_t + Gn_a \qquad (1)$$

Here the term x_{t+1} is a new state at timestamp t+1,
ΔT is the difference in time between the time t and t + 1
x_t is the previous version of t

The acceleration n_a is modelled based on the standard deviation σ_a and noise ratio that may be utilised to reduce the acceleration rate between the two different times. Each particle weight is assigned on the basis of timestamp with regards to the particle movement model. Let us consider ranging error has Gaussian distributions. The weights of the particles may be obtained using equation (2), where $n \in [1, N]$. Here, N represents the total particles. μ_i and σ_i are the calculated range and the standard deviation for the ith measurement, respectively.

$$f(x|\mu, \sigma) = \frac{1}{\sigma\sqrt{2\pi}} exp \frac{-(x-\mu)^2}{2\sigma^2} \qquad (2)$$

$$\omega_n = \prod_{i=1}^{M} f(x_{n,i}|\mu_i, \sigma_i) \qquad (3)$$

Here the term μ - measured range,
x – The range between the anchor and the particle.
σ - SD of the error range
M – The measured variables available
$x_{n,i}$ - the seperation between the nth particle and the anchor that corresponds with the ith measurement,

A.   Timing Acquisition Method

The Timing Acquisition Method is based on a detection method. It is usually analysed the candidate phase by first getting correlation measurements between the template signal (locally generated) and received signal where the template signal balances the stages of the candidate [15]. The correlation measurement is then compared to the threshold for decision making. Such candidate phases can be assessed on a parallel, serial or hybrid basis. For UWB acquisition, many systems depend on detection. Among that, some system focused on creating effective search techniques, which quickly evaluates the search space of the candidate phases. Some other systems suggest two-stage methods of acquisition to reduce the search space itself. The timing estimation is generally acquired by increasing the statistics over a set of candidate phases in the estimation-based methods. Typically, this statistic is extracted from the received signal correlation with the template signal [16].

In wireless communication systems, the timing synchronisation usually relies on the sliding correlators between the transmit clean waveform template and the received signal. Moreover, this method takes a long time to synchronise, accrues high computational complexity and sub-optimum in the existence of a dense multipath. Recently, multiple timing algorithms for UWBIR systems were proposed. They are the Coded-beacon sequence together with a correlators bank approach, transmitted reference (TR) approaches, and the inherent Cyclo Stationarity (CS) method [17]. Every solution works as per these assumptions:

- The lack of multiple paths
- The shortage of TH (time-hopping) codes
- The multi-path channel is identified
- Longer synchronisation time and higher computational complexity
- Bandwidth and power efficiency loss
- The reduction of power efficiency and bandwidth

Timing acquisition in the UWB structure is a particularly difficult task. It is due to insufficient transmitted power and multipath high-resolution. Low transmission power requires a long searching time for reliable synchronisation. If the signal is received with the muti-path components, then the outcome will be in many phases with the search interval. Further, it makes the decision far more complicated. In general, time acquisition is not a new issue in the system of UWB. But it is a significant limitation in receiver design [18].

At the receiver,
$r_{(t)}$ – used to detect the received signal
n_s– Used to identify the symbol-level offset
Where ns is accomplished utilising the timing acquisition algorithms that are supported by DT data.

M_1 - training symbols were sent which has the same value $\{s[k] = 1\}_{k=0}^{M_1-1}$, thus M_1 received during $[\tau_0, \tau_0 + M_1 T_s]$. The first process is to track N ($>M_1$-1) that is the received waveform sections of time T_s.

Under miss of timing $(\tau_0 \neq 0)$, the any Ts-long received section of r(t) could be described as two consecutive parts of symbols, as stated below,

_____

$$x(t + nT_s)$$
$$= w(t + nT_s)$$
$$+ \begin{cases} \sqrt{\varepsilon_s}s[n - n_s - 1]p_R(t + T_s - n_f T_f - \epsilon): t\epsilon[0, n_f T_f \cdot \\ \sqrt{\varepsilon_s}s[n - n_s]p_R(t - n_f T_f - \epsilon) \qquad : t\epsilon[n_f T_f + \epsilon, \end{cases} \quad (4)$$

Where $x_{(t)}$ - received a section of time T_s. The following stage is to accomplish the cross-correlation to produce neighbouring section$R_{x,x}$, as below:

With the occurrence of the training symbols M_1, the consecutively received symbol has similar values. The optimal $\hat{n}_s$ could be evaluated through a line-search for increasing the objective function $J(n_s)$[19] as below:

$$R_{x,x}[n] = \int_0^{T_s} x(t + nT_s)x(t + (n+1)T_s)dt$$
$$= \breve{\omega}[n]$$
$$+ A \int_0^{T_s} P_R^2(t + T_s - n_f T_f - \epsilon)dt$$
$$+ B \int_0^{T_s} P_R^2(t - n_f T_f - \epsilon)dt \quad (5)$$
$$= \breve{\omega}[n] + A \int_{T_s - n_f T_f - \epsilon}^{T_s} P_R^2(t)dt + B \int_0^{T_s - n_f T_f - \epsilon} P_R^2(t)dt.$$

$$Where: \begin{cases} A = \varepsilon_s s[n - n_s - 1].s[n - n_s] \\ B = \varepsilon_s s[n - n_s].s[n - n_s + 1] \end{cases}$$

$$\hat{n}_s = \frac{\max}{n_s \epsilon[0, N - M_1]} J(n_s),$$
$$= \frac{1}{M_1 - 1}\left(\sum_{n=n_s}^{n_s + M_1 - 1} R_{x,x}[n]\right)^2 \quad (6)$$

The occurrence of $r_{(t)}$ in the receiver is avowed when $J(\hat{n}_s) \geq {}^\eta$, Where η the optimal probability of false alarm (FA) is set at a threshold. When the training symbols (M_1) size increases, then its support to integrate the effects of additive noise and help to increase the performance of the synchronisation, but this will reduced bandwidth price and energy efficiency. [20]

B. Synchronisation

The advantage of ultra-wideband (UWB) communication systems is high Ultra-wideband (UWB) communication systems benefit from higher data density by transmitting shorter pulses and lower duty cycles. The strict power restrictions and shorter durations of pulse make UWB output more susceptible to timing errors. Hence, synchronisation of time brings more challenge in these systems [21]. TR modulation has addressed the issue of narrow and low-powered synchronisation to some extent. Removing the need for a specific pulse with locally generated models avoids the extreme synchronisation requirements available in traditional pulse detection methods [22], [23] a. But in the existence of channel noise, the performance of the TR receivers largely depends on accurate timing acquisition

and monitoring of the integration window.

C. TR-UWB and FSR-UWB

In this study, the baseband ultra-wideband system is considered. The symbol interval for TR-UWB systems is specified as T_s and the display interval as T_f. Every frame period has an impulse for UWB, and $T_s = N_f T_f$, N_f "1. In the traditional TR-UWB system in the lth symbol period, the transmission signal can be defined as below,

$$x_{TR}(t) = \sum_{k=0}^{N_f - 1} \left(\sqrt{\frac{E_s}{2}}p(t - lT_s - kT_f) + b_l\sqrt{\frac{E_s}{2}}p(t - lT_s - kT_f - D) \right) \quad (7)$$

Where E_s - transmitted energy per symbol period
$b_l \in \{-1, +1\}$ - information bit to be transmitted during the l$_{th}$ symbol period.
P (.) - normalised UWB pulse shape and is the delay between reference and data pulse.

The requirement for a locally generated reference (LGR) and the complex issue of LGR sync can be eliminated by transmitting a link (reference) with the data. Because TR systems use the portion of the energy output for the signal's reference part, The elimination and difficulty of LGR are at the expense of losing the potential for data transmission [24].

To prevent the recipient's wideband delay feature, Goeckel and Zhang,[25] and Zhang and Goeckel,[26], has been suggested the marginally frequency-shifted reference (FSR) system of UWB. It is much easier to develop a wideband frequency translation signal than the latency of the similar signal. The strategy is used very carefully to choose a frequency translation reference. In other phrases, the reference is translated among frequency instead of time to the data-bearing signal, thereby eliminating the factor of delay. There is no need to enforce the reference and data signal orthogonality over each frame time, even over a symbol period. A frequency offset is therefore proposed between the input data and the reference impulse train, which is just the reverse of symbol duration. Far below the channel's reliability level, the frequency shift is positioned and, therefore, an accurate approximation of the data-bearing signal. Because the data pulse and reverse pulse will traverse precisely in the same channel, the frequency orthogonality obtained by merely moving the pulse pulse is meaningless even though the frequency difference among the pulses exceeds every rational fading channel's consistency rate. Therefore, an orthogonal reference is acquired by the technique with a mixer.

A simple model signal could be described in the FSR-UWB method as x(t), consisting of a generic pulse form with

_____

unmodulated Nf UWB pulses form $x(t) = \sum_{k=0}^{N_f-1} p(t - k\,T_f)$.

The reference waveform is a proportionate x(t) version. A frequency-shifted version of this signal that is generally orthogonal to it across the long Nf symbol period is considered to represent the data waveform. Establishing f0= $1/T_s$ as the frequency shift between the data signal and the reference, the signal transmitted can be represented as[27],

$$x_{FSR}(t) = \sum_{k=0}^{N_f-1} \left(\sqrt{\frac{E_s}{2}} p\left(t - lT_s - kT_f\right) \right.$$
$$+ b_l\sqrt{E_s}p\left(t - lT_s\right)$$
$$\left. - kT_f\right)\cos(2\pi f_0 t) \right) \tag{8}$$

The probability of flaw across a multipath fading channel for the suggested system is

$$P_{FSR-UWB,MP}$$
$$= E_h\left[Q\left(\frac{E_s \sum_{l=0}^{L-1} h_l^2 \cos(2\pi f_0 T_l)}{\sqrt{\frac{5}{2}E_s N_0 \sum_{l=0}^{L-1} h_l^2 + T_s N_0^2 W}} \right) \right] \tag{9}$$

Thus the mathematical justification is derived for attaining the lowest possible frequency difference among reference signals and data signals. The probability error ratio for the generic TR-UWB model is,

$$P_{TR-UWB,MP}$$
$$= E_h\left[Q\left(\frac{E_s \sum_{l=0}^{L-1} h_l^2}{\sqrt{4E_s N_0 \sum_{l=0}^{L-1} h_l^2 + 2T_s N_0^2 W}} \right) \right] \tag{10}$$

Where $E_h[.]$ is the channel-impulse response assumption[25].

To create the symbol timing δ in the system of FSR-UWB, the key have the capability. One technique of showing the scheme's capacity to be synched to demonstrate a quantity dependent on the output occurs, if reduced as a feature of π, resulting in the correct symbol timing. Therefore, it is possible to use adaptive algorithms to reduce these quantities and achieve the right timing.

For $\delta \in [0, T_s]$, define the receiver output as

$$\Lambda(\delta) = \int_{\delta}^{T_s+\delta} r^2(t)\sqrt{2} \cos(2\pi f_0(t-s))\, dt \tag{11}$$
$$= \Lambda_s(\delta) + \Lambda_n(\delta)$$
$$\Lambda_s(\delta) = \int_{\delta}^{T_s+\delta} (h(t) * x(t))^2\sqrt{2} \cos(2\pi f_0(t-\delta))\, dt \tag{12}$$

$$\Lambda_n(\delta) = \int_{\delta}^{T_s+\delta} (n^2(t) + 2(h(t)$$
$$* x(t)) \times \sqrt{2}\cos(2\pi f_0(t-\delta))\, dt \tag{13}$$

It is the approximately Gaussian noise component.

Essential trigonometric functions could be used for Gaussian noise channels to demonstrate that there is zero mean and variance provided by any specified index $\delta \Lambda_s(\delta)$,

$$E[\Lambda_s^2(\delta)] = \left[\frac{1}{2} + \frac{1}{4\pi^2} + \frac{\delta}{T_s} + \frac{\delta^2}{T_s^2}\right]$$
$$+ E_s^2\left[\left(\frac{1}{2} - \frac{1}{4\pi^2} - \frac{\delta}{T_s}\right.\right.$$
$$+ \frac{\delta^2}{T_s^2}\right)\cos(4\pi f_0\,\delta)$$
$$\left.+ \frac{1}{2\pi}\left(\frac{2\delta}{T_s} - 1\right)\sin(4\pi f_0\delta)\right] \tag{14}$$

This has a low-frequency concept(Eqn. 11) δ=0, and δ= T_s are the two peaks we have, and a term (Eqn. 12) is 2 f_0 for frequency. Λn (δ) can be interpreted as having zero variance and mean given by the noise expression,

$$E[\Lambda_n^2(\delta)] = T_s W N_0^2 + 2E_s N_0$$
$$+ \frac{1}{2}\cos(4\pi f_0\,\delta)E_s N_0 \tag{15}$$
$$E[\Lambda^2(\delta)] = E[\Lambda_s^2(\delta)] + E[\Lambda_n^2(\delta)] \tag{16}$$

A low-frequency is also required; it is not based on δ and the frequency period2f0. Furthermore, it is unrelated between the Λ_s (δ) and Λ_n (δ). Consequently, Λ (δ) has zero mean and variance.

IV. NUMERICAL RESULTS

This section presents simulation results toward evaluating the BER efficiency of the TR- UWB schemesand FSR -UWB schemesby considering with and without particle filter. The input parameter for both with and without particle filter is listed in table 1. In the frequency domain, the data modulated and reference signals are separated at the analogue carrier signal requirement cost.

In the frequency and time domains, the frequency-shifted pulse decays quickly. To examine the effect of fine-tuning and Eb on noise efficiency, Eb / N0 are set to 10 dB.

Table 1: Input initialization

Parameters	TR	FSR
Delay effect	2	2
Frequency Translation/Shift	50	50
Data transmission rate	800 kbps	800 kbps
Frames Count	10	10
SNR	10DB	10DB
Number of particles	5000	5000

_____

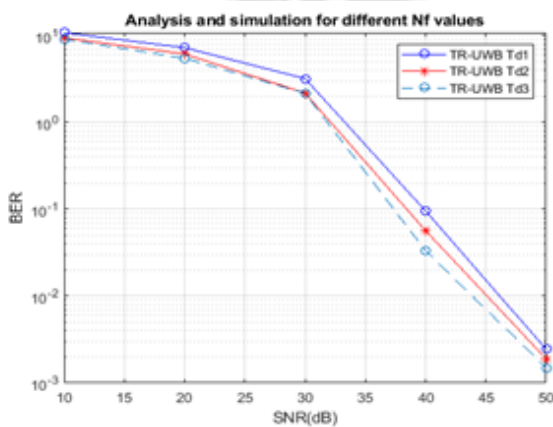### A.   TR-UWB with and without particle filter

The primary objective of the TR-UWB scheme is to recommend a system that evades the delay component on the receiver side. In addition, the frequency-translated comparison is also be chosen depending on the applied frequency conversion of a wideband signal, and this is far easier than the delay signal; the methodology discussed here is used very carefully to select a frequency-translated relationship; in other terms, the frequency (instead of time) relation is interpreted to the data-bearing signal as orthogonal.

The main insight is that these data signals and reference orthogonality must be applied over a symbol period but not over each frame period. A frequency offset between the impulse train of the data and the reference is therefore recommended, which is only the reverse of the duration of the symbol. This frequency paradigm shift is well below the channel frequency consistency to low-data-rate apps that is 100 kb / s and thus serves as a reference for the data-bearing signal as required.   In the research, we introduce and characterises the particle filter system using this probably marginally frequency-shifted reference (FSR) UWB.

Table 2 Effect of delay (Td)

SNR	Without filter			With particle filter		
	BER			BER		
	T_{d1}	T_{d2}	T_{d3}	T_{d1}	T_{d2}	T_{d3}
10	10.8279	9.4386	9.1000	9.7451	8.4947	8.1900
20	7.2648	6.1486	5.4869	6.5383	5.5337	4.9382
30	3.1986	2.1785	2.1700	2.8787	1.9607	1.9530
40	0.0956	0.0567	0.0333	0.0860	0.0510	0.0300
50	0.00245	0.0019	0.0015	0.0022	0.0017	0.0014

The above table 2shows effect of different time delays on the performance. In both the parts it can be noted that with increase in SNR, the BER decreases for all.
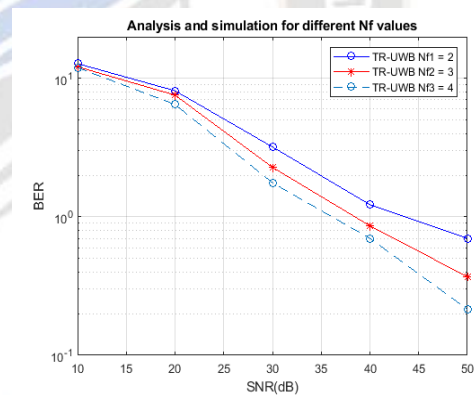

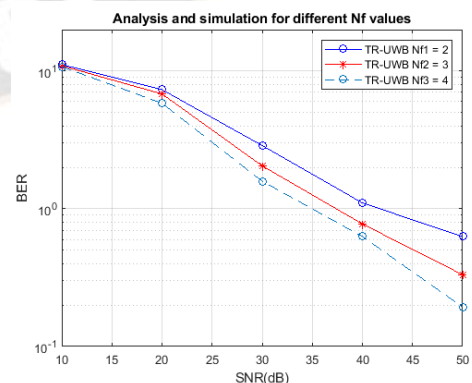**(a) Without particle filter**
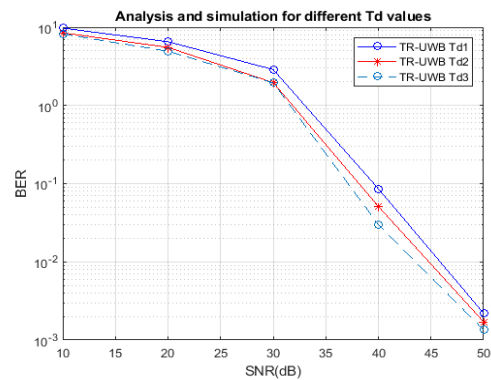
(b) With particle filter
Fig 1. **Simulated results for varying delay response**

Table 3Effect of various frames (Nf) response

SNR	Without filter			With particle filter		
	BER			BER		
	$N_{f1} = 2$	$N_{f2} = 3$	$N_{f3} = 4$	$N_{f1} = 2$	$N_{f2} = 3$	$N_{f3} = 4$
10	12.37896	12.1486	11.9687	11.1411	10.9337	10.7718
20	8.1475	7.5812	6.4869	7.3328	6.8231	5.8382
30	3.1986	2.2785	1.7618	2.8787	2.0507	1.5856
40	1.2256	0.8621	0.6987	1.1030	0.7759	0.6288
50	0.6985	0.3689	0.2150	0.6287	0.3320	0.1935

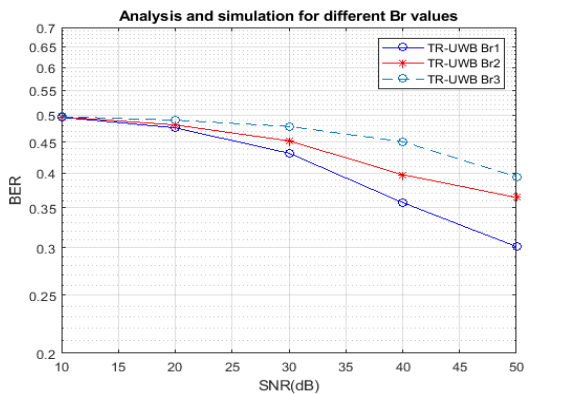**(a) Without particle filter**

(b) With particle filter
Fig 2.Simulated results by considering the number of frame rate

_____

Table 3 provides different frames using SNR's bit error rate. It is evident that when SNR increases, the BER decreases. The BER likewise lowers as the number of frames rises.

In a similar fashion, the table above shows that for various dataspeeds, the bit error rate drops as the SNR increases.

Table 4 Effect of data rate/bit rate (Br)

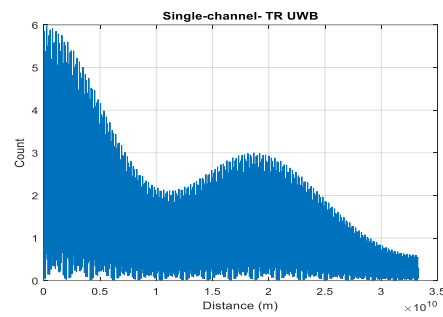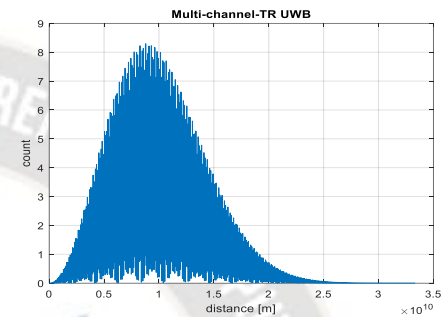| SNR	Without filter			With particle filter		
	BER			BER		
	R_{b1}	R_{b2}	R_{b3}	R_{b1}	R_{b2}	R_{b3}
10	0.4956	0.4964	0.4969	0.4460	0.4468	0.4472
20	0.4758	0.4812	0.4901	0.4282	0.4331	0.4411
30	0.4317	0.4527	0.4784	0.3885	0.4074	0.4306
40	0.3569	0.3974	0.4512	0.3212	0.3577	0.4061
50	0.3014	0.3642	0.3942	0.2713	0.3278	0.3548

(a) Without particle filter
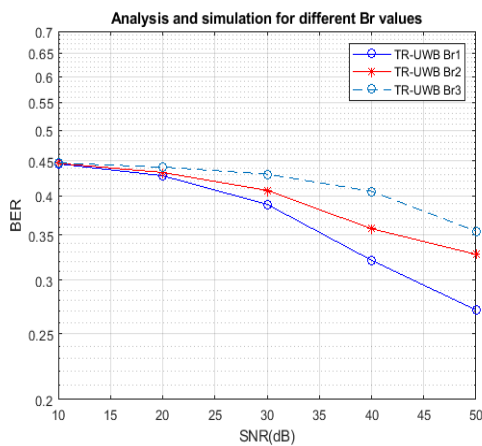
(b) With particle filter

Fig 3. Simulated results by considering various data rate

(a) With particle filter

(b) With particle filter

Fig 4. Simulated results for single and multi-channel conditions

Figure 4 (a) and (b) illustrates that the obtained results of single and multi-channel communication while considering a particle filter. From this, we observed that TR-UWB system with particles filter hires several carries and offers an additional performance increase with carriers compared to the standard TR-UWB of the single-channel system along with the delay line in the receiver. A potential enhancement is the acquisition of frame timing, which might allow the connection interval [0, Ts] to be reduced to specific times that aid the noiseless received signal. This is especially true for Gaussian noise networks or multipath streams with a small delay range.

B. FSR-UWB with and without particle filter

The bit error rate for the SNR for various time delays is shown in Table 5. As the SNR rises, it can be observed that the BER falls. The frequency shift (f0) of the data signal to the reference signal is conveyed during the lth symbol interval. Both the frequency and time domains of the frequency-shifted pulse decrease quite smoothly. To confirm the impact of τ and Eb on the effectiveness of noise, Eb/N0 is set at 10 dB.

Table 5 Effect of frequency shift

SNR	Without filter			With particle filter		
	BER			BER		
	T_{d1}	T_{d2}	T_{d3}	T_{f1}	T_{f2}	T_{f3}
10	8.6376	8.7269	8.3200	6.4967	4.7193	3.6400
20	7.9439	6.2541	6.3414	4.3589	3.0743	2.1948
30	5.2791	2.1986	3.2750	1.9192	1.0893	0.8680
40	1.0561	0.1056	0.06993	0.0574	0.0284	0.0133
50	0.0126	0.0245	0.01280	0.0015	0.0010	0.0006
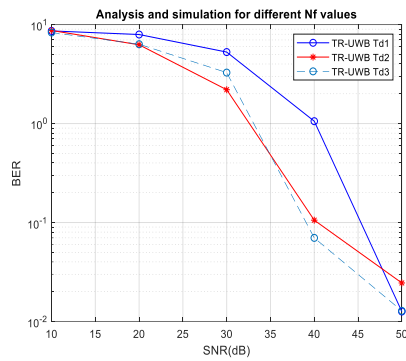
(a) Without particle filter
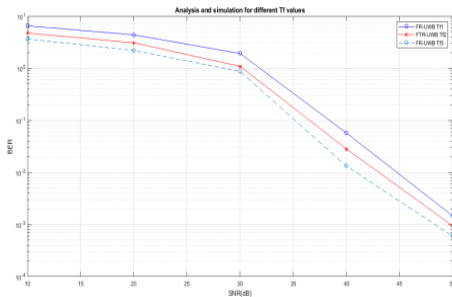
(b) With particle filter

Fig 5. Simulated results for varying delay response

(a) Without particle filter

(b) With particle filter

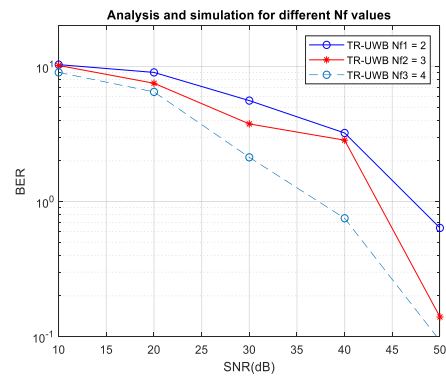**Fig 6. Simulated results for various frame rates**

Figure 5 shows the impact of frequency changes on BER, when the receiver noise bandwidth is set at 600 MHz. We can see from the simulated results that the potential energy detention period was lowered to 30 in order to improve receiver noise performance. The receiver's characteristics are then precisely adjusted to minimize noise performance.

The bit error rate for the SNR for various numbers of frames (Nf) is provided in the table 6. It is evident that when SNR rises, the BER decreases. The BER likewise lowers as the number of frames rises. A Ts = NfTf period of symbol consists of one UWB transmission data pulse and Nf>>1 frame for each length in order to achieve low-data-rate implementations' goals. The results of changing the frame rate while altering the signal to noise ratio from 10 to 50 dB are discussed in Table 6.
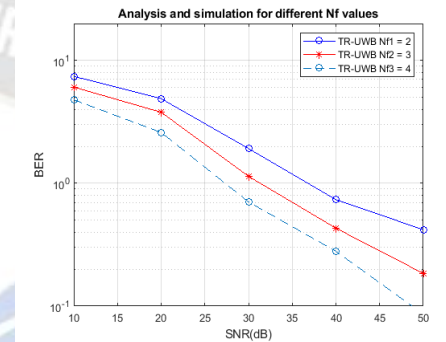
Figure 6 displays the measured FSR-UWB scheme efficiency for various number of frames and Tf=40 ns set frame time on an AWGN channel. Similar to Table 5, Table 6 shows how Bit Error Rate reduces when SNR rises for various number of frames.

Table 6: Effect of the number of frames

SNR	Without filter			With particle filter		
	BER			BER		
	N_{f1}	N_{f2}	N_{f3}	N_{f1}	N_{f2}	N_{f3}
10	10.3260	10.1789	9.0432	7.4274	6.0743	4.7875
20	9.0435	7.5157	6.4869	4.8885	3.7906	2.5948
30	5.5916	3.7568	2.1249	1.9192	1.1393	0.7047
40	3.2191	2.8461	0.7516	0.7354	0.4311	0.2795
50	0.6375	0.1397	0.0931	0.4191	0.1845	0.0860

Table 7: Effect of data rate/bit rate (Rb)

SNR	Without filter			With particle filter		
	BER			BER		
	R_{b1}	R_{b2}	R_{b3}	R_{b1}	R_{b2}	R_{b3}
10	0.4398	0.4290	0.4331	0.4291	0.4130	0.3938
20	0.4213	0.4190	0.4219	0.4136	0.3991	0.3811
30	0.4131	0.3844	0.3527	0.4096	0.3731	0.3312
40	0.3969	0.3592	0.3168	0.3714	0.3497	0.3263
50	0.3200	0.3109	0.2816	0.3169	0.3009	0.2509

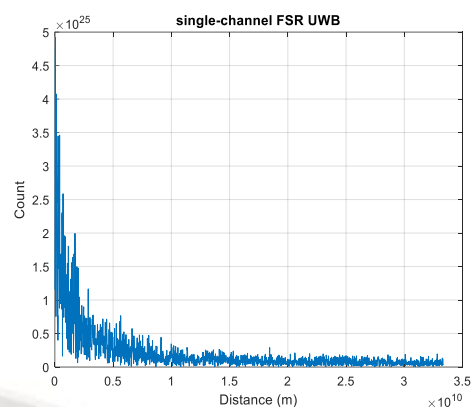**(a) Without particle filter**

_____
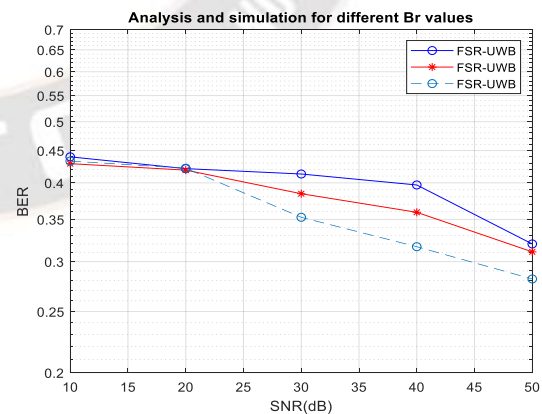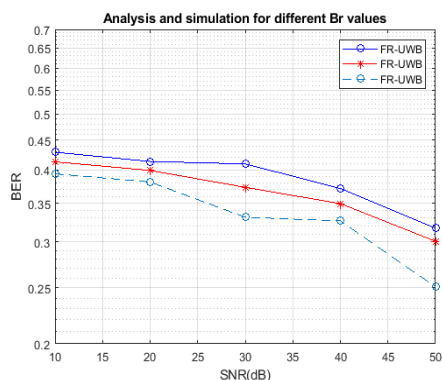
(b) With particle filter

**Fig 7. Simulated results by considering various data rate**

Figure 7 compares the data rates of UWB technology to those of other wireless technologies. Table 7 contains the acquired SNR (10 to 50) to data rate findings. We simulated a high data rate UWB communication using Tf = 4, 6 ns,and data rate 30 Mbit/s and 25 Mbit/s. When data rate increases (Tf = 6 ns), the advantage of an optimised code series arrangement becomes clear and leads to better noise, data rate, and delay performance.

The presented system's BER performance is examined in a variety of multi-path channel scenarios. Even in the case of a transmission system with several paths, the suggested approach can minimise the bit error rate. To fine-tune the timing and frequency domain equalisation coefficients, it depends on the impulse response of timing error. Synchronization with the channel estimation function is made possible by this structure in conjunction with the preface overhead. In the end, the FSR-UWB system's single path and multipath channel circumstances are used to compare the findings.

Figure 8a shows the statistical behavior of single-channel and multi-channel communication systems. The single-channel system's variance is spread out considerably. Additionally, the mean single-channel offset is greater than the mean offset for the multi-channel technique. In Figure 8b, standard deviation (sd) is comparable to that of Figure 8a. But, only spread slightly increased due to the change in frequency.
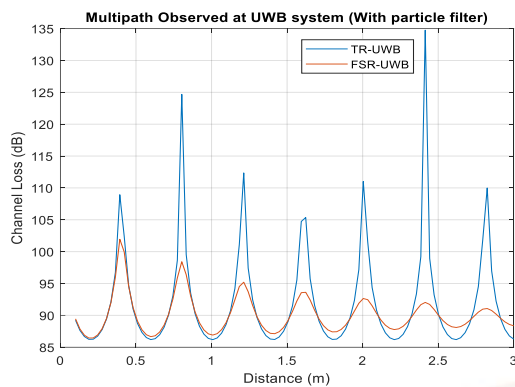
(a) With particle filter
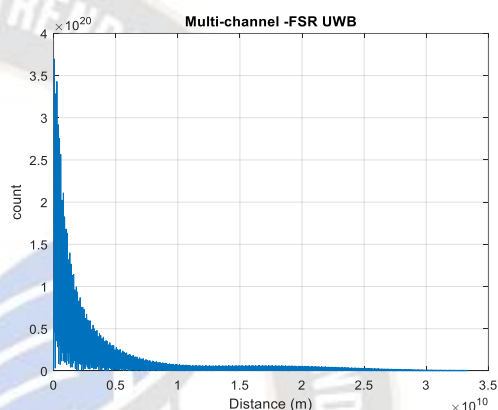
(b) With particle filter

**Fig 8. Simulated results for single and multi-channel conditions**

Because there is no delay line from the receiver line, an FSR-UWB system employs multiple carriers and performs even better than the FSR-UWB reference system. The possible improvement, especially for small delay spread AWGN or multipath channels, is to gain frame synchronisation such that the connection interval $[\ 0,\ T_s\ ]$. Certain phases for which the received noiseless signal is allowed could be reduced.

C.   Multipath Effect

During the implementation, the multi-path components are captured via a received signal that enhances the system performance when relations with the conventional TR-UWB system by performing multi-path diversity or number of correlators. The performance of multi-path channel communication has been observed in both the UWB system, TR and FSR, with and without particle filter. The results are illustrated in figure 9 (a) and 9(b).

_____

(a) Observed results while considering with particle filter
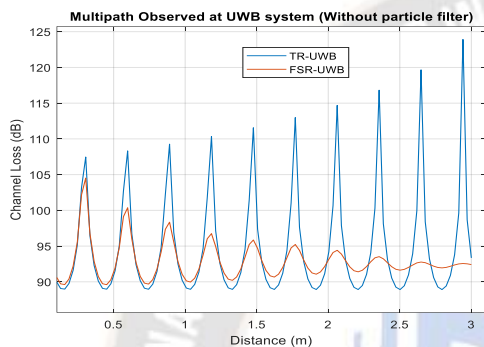
(b) Observed results while considering with particle filter
Fig 9. Multipath Observed results at UWB System

Some signals may come via reflections to the destination through various paths and could even boost productively or destructively. This multi-path impact may trigger the received signal to have major variations. To test the power loss from a simulator, contrast it with the results from the study below and ensure that they suit. Improving the bandwidth of a network improves its channel ability. It allows for higher data levels for UWB applications in communication systems and more comprehensive scope resolutions. The improved bandwidth for both devices may also boost reliability to multipath fading. Wideband systems usually work with such a bandwidth approaching 5% of the centre frequency.

V. CONCLUSION

In this study, TR-UWB and FSR-UWB techniques have been introduced, which provided fine synchronisation and timing error using a tracking loop based particle filter with the acquisition method. The suggested approach increases the transmission rate while considering three different time delay and frequency ranges than the traditional TR-UWB and FSR-UWB without particle filter. Moreover, the performance of the suggested model has been validated in terms of data rate, multi-channel condition, delay and frame rate. The simulation results illustrate that the proposed model of FSR-UWB with particle filter gives better performance over different channel models when relating with the FSR-UWB of without particle

filter and TR-UWB with and the particle filter. Thus the obtained result showed a reduction in the receiver complexity and increased the date rate with fine synchronisation.

REFERENCES

[1] Darif, A., Saadane, R., & Aboutajdine, D. (2014). Performance Evaluation of WideMac Compared to ALOHA in term of Energy Consumption for IR-UWB based WSN. *Journal of Emerging Technologies in Web Intelligence*, *6*(1). https://doi.org/10.4304/jetwi.6.1.54-58.

[2] Zaki, A. I., Badran, E. F., & El-Khamy, S. E. (2016). Two Novel Space-Time Coding Techniques Designed for UWB MISO Systems Based on Wavelet Transform. *PLOS ONE*, *11*(12),e0167990.https://doi.org/10.1371/journal.pone.0167990

[3] Charlier, M., Quoitin, B., & Hauweele, D. (2019). Challenges in using time slotted channel hopping with ultra wideband communications. In *Proceedings of the International Conference on Internet of Things Design and Implementation - IoTDI '19* (pp. 82–93). New York, New York, USA: ACM Press. https://doi.org/10.1145/3302505.3310071

[4] Banstola, R., Bera, R., & Bhaskar, D. (2013). Review and Design of UWB Transmitter and Receiver. *International Journal of Computer Applications*, *69*(13), 25–28. https://doi.org/10.5120/11903-7978

[5] Mohammed, M. S., Singh, M. J., & Abdullah, M. (2017). New TR-UWB Receiver Algorithm Design to Mitigate MUI in Concurrent Schemes. *Wireless Personal Communications*, *97*(3), 4431–4450. https://doi.org/10.1007/s11277-017-4732-z

[6] Umek, A., Tomažič, S., & Kos, A. (2019). Application for Impact Position Evaluation in Tennis Using UWB Localization. *Procedia Computer Science*, *147*, 307–313. https://doi.org/10.1016/j.procs.2019.01.269

[7] Ray, K. P., & Thakur, S. S. (2019). Modified Trident UWB Printed Monopole Antenna. *Wireless Personal Communications*. https://doi.org/10.1007/s11277-019-06646-x

[8] Torino, P. D. I. (2019). Repository ISTITUZIONALE A Useful Approximation to Add up Contributions in Ray Based EM Propagation Algorithms Session 3AP Poster Session 2, (September). Retrieved from https://iris.polito.it/retrieve/handle/11583/1958813/51313/3AP.pdf#page=16

[9] Huo, Y., Dong, X., & Lu, P. (2017). Ultra-wideband transmitter design based on a new transmitted reference pulse cluster. *ICT Express*, *3*(3), 142–147. https://doi.org/10.1016/j.icte.2017.07.001

[10] Liang, Z., Zhang, G., Dong, X., & Huo, Y. (2018). Design and Analysis of Passband Transmitted Reference Pulse Cluster UWB Systems in the Presence of Phase Noise. *IEEE Access*, *6*, 14954–14965. https://doi.org/10.1109/ACCESS.2018.2815708

[11] Djapic, R., Leus, G., & van der Veen, A. (2005). Synchronization and Detection for Transmitted Reference

278

_____

UWB Systems. In *Conference Record of the Thirty-Ninth Asilomar Conference onSignals, Systems and Computers, 2005.* (pp. 1084–1088). IEEE. https://doi.org/10.1109/ACSSC.2005.1599926

[12] Franz, S., & Mitra, U. (2006). Generalized UWB transmitted reference systems. *IEEE Journal on Selected Areas in Communications*, 24(4), 780–786. https://doi.org/10.1109/JSAC.2005.863829

[13] Yi-Ling Chao, & Scholtz, R. A. (2004). Optimal and suboptimal receivers for ultra-wideband transmitted reference systems. In *GLOBECOM '03. IEEE Global Telecommunications Conference (IEEE Cat. No.03CH37489)* (Vol. 2, pp. 759–763). IEEE. https://doi.org/10.1109/GLOCOM.2003.1258340

[14] Gifford, W. M., & Win, M. Z. (2004). On transmitted-reference UWB communications. In *Conference Record of the Thirty-Eighth Asilomar Conference on Signals, Systems and Computers, 2004.* (Vol. 2, pp. 1526–1531). IEEE. https://doi.org/10.1109/ACSSC.2004.1399410

[15] Sibbett, T., Moradi, H., & Farhang-Boroujeny, B. (2016). Novel Maximum-Based Timing Acquisition for Spread-Spectrum Communications. In *2016 IEEE Globecom Workshops (GC Wkshps)* (pp. 1–7). IEEE. https://doi.org/10.1109/GLOCOMW.2016.7848972

[16] Han, C., Akyildiz, I. F., & Gerstacker, W. H. (2017). Timing Acquisition and Error Analysis for Pulse-Based Terahertz Band Wireless Systems. *IEEE Transactions on Vehicular Technology*, 66(11), 10102–10113. https://doi.org/10.1109/TVT.2017.2750707

[17] Liu, Y., Wu, Q., Zhang, Y., Gao, J., & Qiu, T. (2019). Cyclostationarity-based DOA estimation algorithms for coherent signals in impulsive noise environments. *EURASIP Journal on Wireless Communications and Networking*, 2019(1), 81. https://doi.org/10.1186/s13638-019-1410-8

[18] Kroll, H., Korb, M., Weber, B., Willi, S., & Huang, Q. (2017). Maximum-Likelihood Detection for Energy-Efficient Timing Acquisition in NB-IoT. In *2017 IEEE Wireless Communications and Networking Conference Workshops (WCNCW)* (pp. 1–5). IEEE. https://doi.org/10.1109/WCNCW.2017.7919084

[19] Shen, X. (Sherman), Guizani, M., Caiming, R., Le-Ngoc, & Tho, Q. and. (2006). *Ultra-Wideband Wireless Communications And Networks*. *Wireless Communications*. Retrieved from http://read.pudn.com/downloads226/ebook/1061232/W C and Networks by MD/2072-0470011440.pdf

[20] Huang, T.-J., & Yang, J.-F. (2017). An Effective Timing Synchronization Scheme for DHTR UWB Receivers. *Wireless Personal Communications*, 95(4), 3495–3508. https://doi.org/10.1007/s11277-017-4009-6

[21] Yorio, Z. (2020). Improving a wireless localization system via machine learning techniques and security protocols. Retrieved from https://commons.lib.jmu.edu/cgi/viewcontent.cgi?article=10 71&context=masters202029

[22] Qiu, Y., Yang, Q., Deng, M., & Chen, K. (2020). Time synchronization and data transfer method for towed electromagnetic receiver. *Review of Scientific Instruments*, 91(9), 094501. https://doi.org/10.1063/5.0012218

[23] Prager, S., Haynes, M. S., & Moghaddam, M. (2020). Wireless Subnanosecond RF Synchronization for Distributed Ultrawideband Software-Defined Radar Networks. *IEEE Transactions on Microwave Theory and Techniques*, 68(11), 4787–4804. https://doi.org/10.1109/TMTT.2020.3014876

[24] Zhang, Z., Li, J., & Yang, X. (2020). Data Aggregation in Heterogeneous Wireless Sensor Networks by Using Local Tree Reconstruction Algorithm. *Complexity*, 2020, 1–14. https://doi.org/10.1155/2020/3594263

[25] Goeckel, D. L., & Zhang, Q. (2007). Slightly Frequency-Shifted Reference Ultra-Wideband (UWB) Radio. *IEEE Transactions on Communications*, 55(3), 508–519. https://doi.org/10.1109/TCOMM.2007.892452

[26] Zhang, Q., & Goeckel, D. L. (2007). Multiple-Access Slightly Frequency-Shifted Reference Ultra-Wideband Communications for Dense Multipath Channels. In *2007 IEEE International Conference on Communications* (pp. 1083–1088). IEEE. https://doi.org/10.1109/ICC.2007.184

[27] Zhang, J., Hu, H.-Y., Liu, L.-K., & Li, T.-F. (2007). Code-Orthogonalized Transmitted-Reference Ultra-Wideband (UWB) Wireless Communication System. In *2007 International Conference on Wireless Communications, Networking and Mobile Computing* (pp. 528–532). IEEE. https://doi.org/10.1109/WICOM.2007.138

[28] S. L. Bangare, "Classification of optimal brain tissue using dynamic region growing and fuzzy min-max neural network in brain magnetic resonance images", Neuroscience Informatics, Volume 2, Issue 3, September 2022, 100019, ISSN 2772-5286, https://doi.org/10.1016/j.neuri.2021.100019.

[29] S. L. Bangare, S. Prakash, K. Gulati, B. Veeru, G. Dhiman and S. Jaiswal, "The Architecture, Classification, and Unsolved Research Issues of Big Data extraction as well as decomposing the Internet of Vehicles (IoV)," 2021 6th International Conference on Signal Processing, Computing and Control (ISPCC), 2021, pp. 566-571, doi: 10.1109/ISPCC53510.2021.9609451.

[30] S. L. Bangare, A. R. Khare, P. S. Bangare, "Code parser for object Oriented software Modularization", International Journal of Engineering Science and Technology, ISSN: 0975-5462, Vol. 2 (12), 2010, 7262-7265..

[31] Suneet Gupta, Sumit Kumar, Sunil L. Bangare, Shibili Nuhmani, Arnold C. Alguno, Issah Abubakari Samori, "Homogeneous Decision Community Extraction Based on End-User Mental Behavior on Social Media", Computational Intelligence and Neuroscience, vol. 2022, Article ID 3490860, 9 pages, 2022. https://doi.org/10.1155/2022/3490860.

[32] P. S. Bangare, P. N. Gandhi, S. L. Bangare, "The Campus Navigator: An Android Mobile Application", International Journal of Advanced Research in Computer and Communication Engineering, Vol. 3, Issue 3, March 2014, Page(s) 5715-5717, ISSN (Online) : 2278.

_____

[33] Xu Wu, Dezhi Wei, Bharati P. Vasgi, Ahmed Kareem Oleiwi, Sunil L. Bangare, and Evans Asenso, "Research on Network Security Situational Awareness Based on Crawler Algorithm", Security and Communication Networks, Hindawi, ISSN:1939-0114, E-ISSN:1939-0122, https://www.scopus.com/sourceid/18000156707.

[34] Ajay S. Ladkat, Sunil L. Bangare, Vishal Jagota, Sumaya Sanober, Shehab Mohamed Beram, Kantilal Rane, Bhupesh Kumar Singh, "Deep Neural Network-Based Novel Mathematical Model for 3D Brain Tumor Segmentation", Computational Intelligence and Neuroscience, vol. 2022, Article ID 4271711, 8 pages, 2022. https://doi.org/10.1155/2022/4271711.

[35] L.M.I. Leo Joseph, S.L. Bangare, et al., Methods to identify facial detection in deep learning through the use of real-time training datasets management, Efflatounia (ISSN 1110-8703) 5 (2) (2021) 1298–1311.